Japanese Journal of Radiology (2019) 37:735–749
https://doi.org/10.1007/s11604-019-00867-7

INVITED REVIEW

Neuroimaging of Alzheimer's disease: focus on amyloid and tau PET

Hiroshi Matsuda[1] · Yoko Shigemoto[2] · Noriko Sato[2]

Received: 23 July 2019 / Accepted: 28 August 2019 / Published online: 6 September 2019

Abstract
Although the diagnosis of dementia is still largely a clinical one, based on history and disease course, neuroimaging has dramatically increased our ability to accurately diagnose it. Neuroimaging modalities now play a wider role in dementia beyond their traditional role of excluding neurosurgical lesions and are recommended in most clinical guidelines for dementia. In addition, new neuroimaging methods facilitate the diagnosis of most neurodegenerative conditions after symptom onset and show diagnostic promise even in the very early or presymptomatic phases of some diseases. In the case of Alzheimer's disease (AD), extracellular amyloid-β (Aβ) aggregates and intracellular tau neurofibrillary tangles are the two neuropathological hallmarks of the disease. Recent molecular imaging techniques using amyloid and tau PET ligands have led to preclinical diagnosis and improved differential diagnosis as well as narrowed subject selection and treatment monitoring in clinical trials aimed at delaying or preventing the symptomatic phase of AD. This review discusses the recent progress in amyloid and tau PET imaging and the key findings achieved by the use of this molecular imaging modality related to the respective roles of Aβ and tau in AD, as well as its specific limitations.

Keywords Dementia · Alzheimer's disease · PET · Amyloid · Tau

Introduction

Alzheimer's disease (AD) is an irreversible, progressive brain disorder that slowly compromises the healthy brain, affecting memory, cognitive skills, emotions, behavior, and mood. Over time, a person's ability to carry out daily activities becomes impaired. AD is the most common form of dementia, accounting for around two-thirds of cases [1]. The 2018 World Alzheimer Report [2] indicated that there were 50 million people living with dementia worldwide, with the number of cases projected to almost double every 20 years. In Japan, a 2013 study commissioned by the Ministry of Health, Labour, and Welfare reported that more than 4.6 million Japanese were living with dementia. This number is expected to reach 7 million in 2025, representing approximately one in five elderly people in Japan [3].

Criteria for the clinical diagnosis of AD were established by a workgroup of the National Institute of Neurological and Communicative Disorders and Stroke and the Alzheimer's Disease and Related Disorders Association in 1984 [4]. These criteria were universally adopted, have been extremely useful, and have survived intact without modification for well over a quarter of a century. However, the intervening 35 years have seen advances in the understanding of AD and our ability to detect its pathophysiological process, as well as changes in conceptualization regarding the clinical spectrum of the disease. The pathophysiological process of AD is thought to begin many years before the diagnosis of AD dementia. This long preclinical phase of AD could provide a critical opportunity for therapeutic intervention. However, we need to further elucidate the link between the pathological cascade of AD and the emergence of clinical symptoms. The National Institute on Aging and the Alzheimer's Association convened an international working group to review the biomarker, epidemiological, and neuropsychological evidence and to develop recommendations to identify the factors that best predict the risk of progression from normal cognition to mild cognitive impairment

✉ Hiroshi Matsuda
matsudah@ncnp.go.jp

[1] Integrative Brain Imaging Center, National Center of Neurology and Psychiatry, 4-1-1 Ogawahigashi, Kodaira, Tokyo 187-8551, Japan

[2] Department of Radiology, National Center of Neurology and Psychiatry, 4-1-1 Ogawahigashi, Kodaira, Tokyo 187-8551, Japan

(MCI) and AD dementia [5, 6]. A conceptual framework and operational research criteria were proposed based on the prevailing scientific evidence, as well as the testing and refinement of these models through longitudinal clinical research studies [7, 8].

The staging of preclinical AD was also proposed [8]. Stage 1 involves asymptomatic amyloidosis with high PET amyloid tracer retention and low cerebrospinal fluid (CSF) levels of the 42-amino acid-long amyloid β (Aβ) peptide ($A\beta_{42}$). Stage 2 has both amyloidosis and neurodegeneration with neuronal dysfunction on ^{18}F-fluorodeoxy glucose (^{18}F-FDG) PET or functional MRI, high CSF tau/phosphorylated tau, and cortical thinning/hippocampal structure atrophy on structural MRI. Stage 3 adds subtle cognitive decline to the amyloidosis and neurodegeneration with evidence of a subtle change from baseline cognition and poor performance on more challenging cognitive tests but does not meet the criteria for MCI.

Patients who are memory impaired but have limited functional impairment and do not meet the clinical criteria for dementia are classified as having MCI or mild neurocognitive disorder as defined in the most recent Diagnostic and Statistical Manual of Mental Disorders V [9–11]. MCI is increasingly recognized as a major health care issue because of its association with significant morbidity, including the development of dementia and AD dementia. MCI is a heterogeneous clinical syndrome, and new criteria for MCI due to AD are intended to help to increase the accuracy of AD diagnosis in the pre-dementia stage [12]. One 5-year longitudinal epidemiological study estimated the rate at which individuals with MCI progress to dementia in Nakayama, Japan [13]. Community dwellers aged 65 years and older were invited to participate over a 14-month period. Overall, the annual conversion rate from MCI to dementia was reported to be 16.1% per 100 person-years, with the conversion rate from MCI to AD dementia 8.5% per 100 person-years. In the Japanese Alzheimer's disease neuroimaging initiative (J-ADNI) study [14], MCI patients (234 patients enrolled, 232 at baseline) progressed to dementia in 12 months at a rate of 28.8%/year, more rapidly than in the ADNI study in the United States (20.2%). The significantly higher rate of conversion to dementia in the J-ADNI persisted until 18 months (39.7% in the J-ADNI vs. 27.4% in the ADNI), whereas the rate in the ADNI caught up after 24 months, reaching 45.1% in the J-ADNI and 40.9% in the ADNI at 36 months. These conversion rates are consistent with those described previously (7–20%) [9–13], with any variations likely to be related to the different measures used to define MCI across the studies.

Due to the recent progress in biomarkers, Jack et al. [15] proposed an unbiased descriptive classification scheme for AD biomarkers. They proposed the "A/T/N" system in which seven major AD biomarkers are divided into three binary categories based on the nature of the pathophysiology that each measures. "A" refers to the value of the Aβ biomarker (amyloid PET or CSF $A\beta_{42}$), "T", the value of the tau biomarker (CSF phosphorylated tau or tau PET), and "N", biomarkers of neurodegeneration or neuronal injury (^{18}F-fluorodeoxyglucose PET, structural MRI, or CSF total tau). Each biomarker category is rated as positive or negative. It is agnostic to the temporal ordering of mechanisms underlying AD pathogenesis and is a descriptive system for categorizing multidomain biomarker findings at the individual level in an easy to understand and use format (Table 1, Figs. 1, 2, 3, 4). Given this situation, the role of amyloid and tau PET is becoming increasingly important. This review presents the current state of these molecular imaging approaches in AD research.

Amyloid PET

PET ligands

One of a number of compounds that have been developed for the imaging of amyloid, *N*-methyl-[^{11}C]2-(4′-methylaminophenyl)-6-hydroxybezothiazole or simply Pittsburgh Compound-B (PiB) [16] is the derivative of the

Table 1 A/T/N classification scheme for AD imaging biomarkes corresponding to NIA-AA classification

A/T/N score	Preclinical AD	MCI	probable AD dementia
A−/T−/N−	Not defined	MCI, unlikely due to AD	Dementia, unlikely due to AD
A+/T−/N−	Stage 1	MCI, core clinical criteria	Intermediate likelihood; probable AD dementia; based on clinical criteria
A+/T+/N−	stage 2/3	MCI, core clinical criteria	High likelihood; probable AD dementia; based on clinical criteria
A+/T−/N+	Not defined	MCI, core clinical criteria	High likelihood; probable AD dementia; based on clinical criteria
A+/T+/N+	stage 2/3	MCI due to AD, high likelihood	High likelihood AD pathophysiology
A−/T+/N−	Not defined	Not defined	Probable AD dementia; based on clinical criteria
A−/T−/N+	Not defined	Not defined	Intermediate likelihood; probable AD dementia; based on clinical criteria
A−/T+/N+	Not defined	Not defined	Intermediate likelihood; probable AD dementia; based on clinical criteria

A amyloid PET, *T* tau PET, *N* FDG-PET or MRI

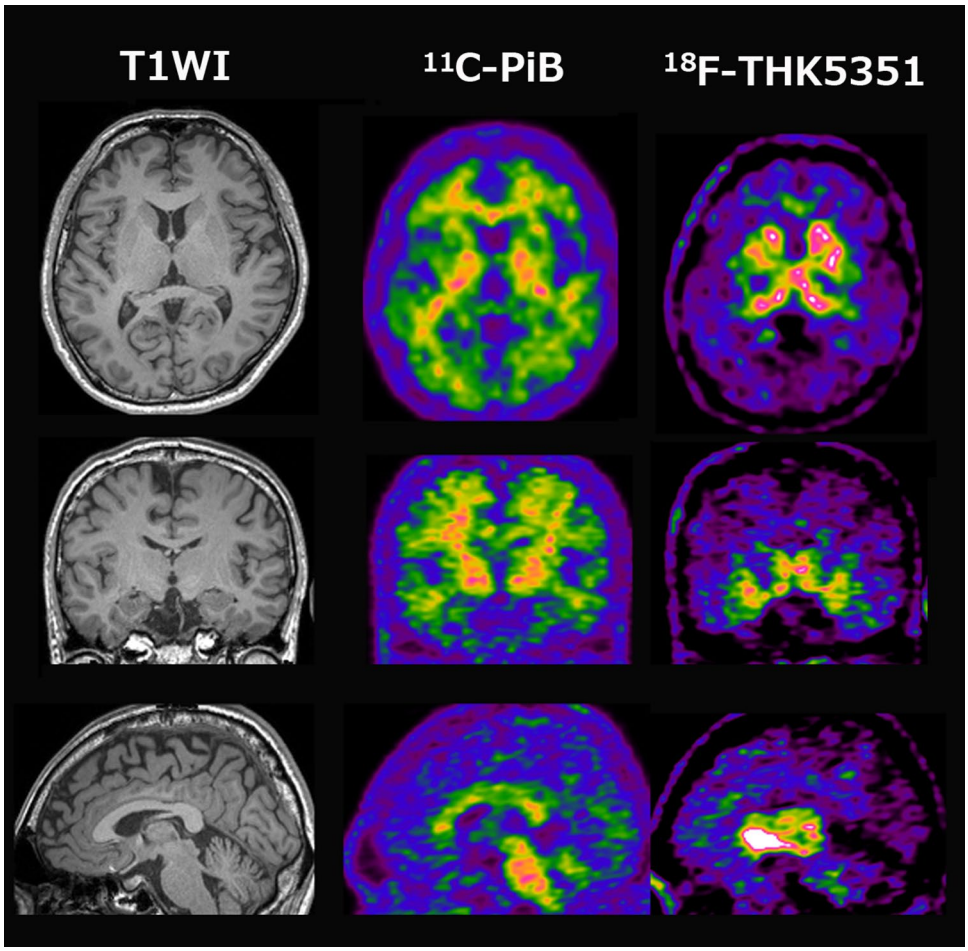

Fig. 1 Cognitively normal individual (A−/T−/N−). ^{11}C-PiB: amyloid (A). ^{18}F-THK5351: tau (T). MRI: neuronal injury (N). All three biomarkers are negative

amyloid-binding dye thioflavin-T and the most extensively validated tracer. It binds to aggregated, fibrillar Aβ deposits, such as those found in the cerebral cortex and striatum, but not to amorphous Aβ deposits, such as those predominating in the cerebellum. The first ^{11}C-PiB PET study in humans [17] was performed in mild AD patients, where the uptake pattern was consistent with the Aβ plaque deposition described in postmortem studies of AD brains. Postmortem studies of patients who showed elevated ^{11}C-PiB deposition during life had high correlations between in vivo ^{11}C-PiB accumulation and in vitro measures of Aβ pathology [18, 19]. However, due to the 20-min half-life of ^{11}C, ^{11}C-PiB can only be used in PET centers with on-site cyclotron and radiopharmacy facilities.

^{18}F is a more suitable radionuclide for widespread clinical use, because its longer half-life of 110 min allows delivery from radiopharmaceutical companies to multiple PET centers. Three ^{18}F-labeled tracers have been developed, whose automated synthesizers are approved by pharmaceutical and medical device law in Japan but not reimbursed. Flutemetamol [20] (Vizamyl, GE Healthcare; synthesized by FASTlab, GE Healthcare) is a close structural analogue of ^{11}C-PiB, whereas florbetapir [21] (Amyvid, Eli Lilly; synthesized by NEPTIS, Eli Lilly, and MPS200Aβ, Sumitomo Heavy Industries) and florbetaben [22] (Neuraceq, Life Molecular Imaging; synthesized by Synthera, SCETI) are derived from stilbene. Marketing authorizations were granted by the pharmaceutical and medical devices agency for flutemetamol (Vizamyl, Nihon Medi-Physics) and florbetapir (Amyvid, Fuji Film Toyama Chemical), which are not reimbursed either in Japan. These ^{18}F-labeled tracers are approved for "Visualization of intracerebral amyloid β plaques in patients with cognitive impairment suspected of Alzheimer's disease". Although ^{11}C-PiB PET images in AD usually show greater binding in gray matter than in white matter, this is not the case for the ^{18}F-labled tracers that will be the mainstay of clinical practice in the near future. All ^{18}F-labeled tracers have high nonspecific white matter uptake, giving a distinctive white matter pattern in scans of amyloid-negative individuals [23]. This negative pattern resembles the smoothed white matter image obtained with the low spatial resolution of PET segmented from whole-brain T1-weighted MRI. In AD, the ^{18}F-labeled tracers frequently show loss of the gray matter–white matter demarcation and consequent loss of the normal white matter pattern as the predominant evidence of cortical amyloid plaque and less often shows

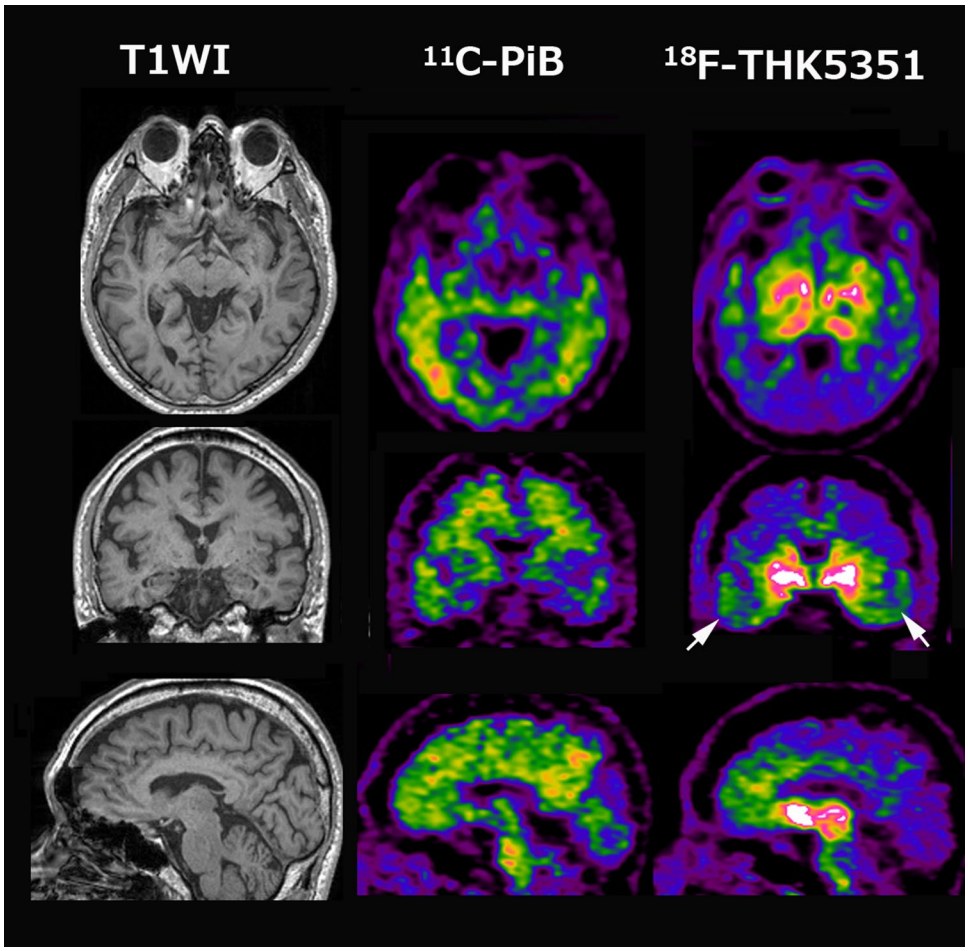

Fig. 2 Individual with preclinical AD (A+/T+/N−). Aβ load is present in the right temporal cortex and precuneus. Tau-related pathophysiology is present in the basal and lateral temporal cortex (arrows). No atrophy is present in medial temporal areas

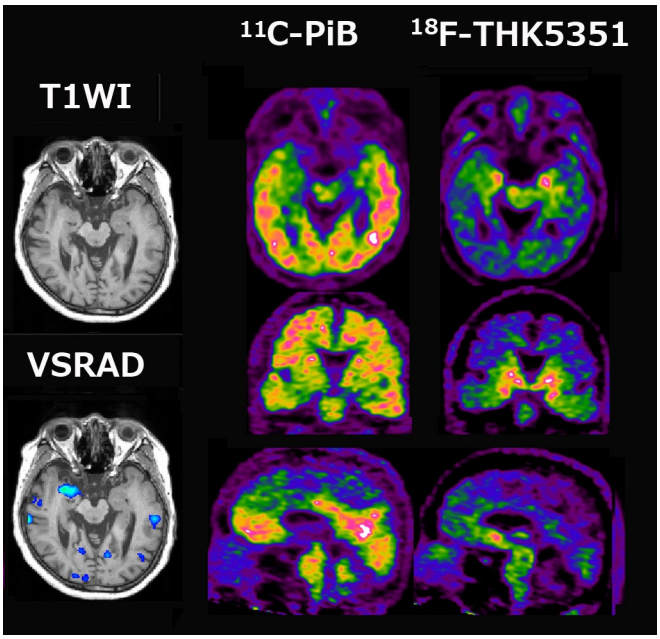

Fig. 3 Individual with MCI due to AD (A+/T+/N+). Voxel-based specific regional analysis system for AD (VSRAD) shows mild right medial temporal lobe atrophy. All three biomarkers are positive

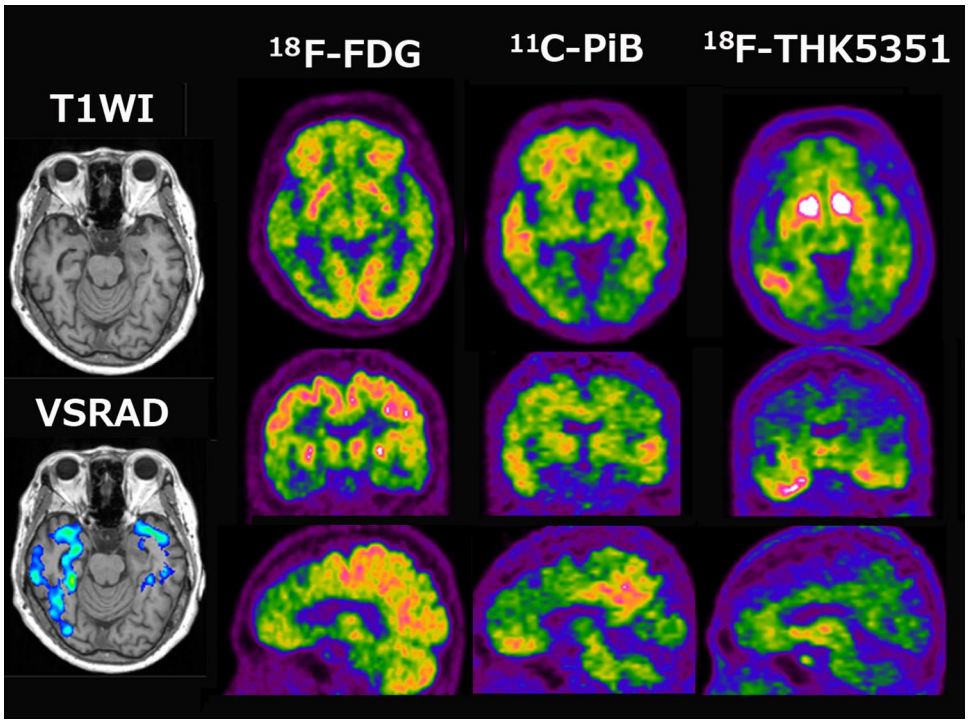

Fig. 4 Individual with AD dementia (A+/T+/N+). VSRAD shows right-side dominant medial and lateral temporal lobe atrophy. All three biomarkers are positive. Cortical tau accumulation is prominent in areas with glucose hypometabolism

the clearly intense binding in the cortical ribbon typical of a positive ^{11}C-PiB scan.

Visual interpretation

A commonly used reading technique for amyloid PET involving visual inspection is to set a color scale with a good dynamic range to the cerebellar white matter or pons and then inspect a midsagittal slice for uptake in the medial orbitofrontal cortex and posterior medial parietal area (posterior cingulate gyrus and precuneus). Transaxial slices are then reviewed for uptake in lateral temporal, parietal, and striatal regions. In a positive scan, five key areas—the medial orbitofrontal, posterior cingulate gyrus/precuneus, striatum, lateral temporal, and parietal gray matter—show increased tracer uptake. In contrast, the cerebellar gray matter shows far less accumulation. The medial temporal region, visual cortex, and primary sensorimotor cortex also show less accumulation. In a negative scan, the midline sagittal slice shows uptake in the corpus callosum and pons, whereas a typical white matter pattern is seen on the transverse side with more marked uptake in the perithalamic area. In addition, there is clear separation of uptake between the left and right hemispheres apart from the white matter connections, as can be seen in the medial orbitofrontal and precuneus areas. Striatal uptake follows cortical uptake in sporadic AD. For visual interpretation of amyloid PET, a three-stage PET classification has been proposed: low cortical; high cortical + low striatal; and high cortical + high striatal [24].

Quantitative assessment

Amyloid PET tracer binding to Aβ plaque in the gray matter is specific and reversible, whereas its binding in the white matter is nonspecific and nonsaturable [25]. The relatively slow kinetics of amyloid PET tracer make the specific uptake in the gray matter prominent at later time points, which may impede the quantification of Aβ deposits with ^{11}C-PiB. To overcome this drawback in quantification, three-dimensional dynamic sampling of emission data for the whole brain is desirable, lasting about 70–90 min after tracer injection. Application of the linear models developed by Logan [26] to these sampling data has become a standard method for robust quantification in ^{11}C-PiB studies. Logan analysis is used to calculate the distribution volume of ligand tracers that have reversible binding kinetics. The selection of the cerebellar cortex as a reference region that has no specific ^{11}C-PiB deposition enables calculation of a distribution volume ratio (DVR) without arterial plasma data sampling as the slope of a graphical plot [27]. The DVR equals binding potential + 1. The pons can also be chosen as a reference area [28]. On the other hand, the standardized uptake value ratio (SUVR) [29] has been proposed as a more feasible semi-quantitative analytical method than the DVR. The SUVR is calculated via computation of the region-to-cerebellum ratio at later timepoints. The advantages of the SUVR approach include large effect sizes for AD and control group differences and the possibility to obtain the required data from a single 20-min scan. The reliability of the SUVR is better

with ^{18}F-labeled tracers than with ^{11}C-PiB because of the higher count rate. The disadvantages of this approach are the slightly lower test–retest variability than in the DVR approach and the potential for time-varying outcomes [29]. The use of a standardized volume of interest template with amyloid PET images spatially normalized to the same standardized space has been provided as an automated voxel-based method for amyloid PET deposition analysis [30].

To overcome the considerable variability of the SUVR due to differences in the PET tracers and PET scanners used, standardization has been proposed for quantitative amyloid imaging measures by scaling the outcome of each particular analysis method or tracer to a 0–100 scale, anchored by young controls and typical AD patients, with the units called "Centiloids" [31]. Regions that share a border with lower- or higher binding structures are susceptible to partial volume effects due to a blurring caused by the low resolution of PET. Because gray matter, white matter, and CSF have different tracer uptake patterns, all gray matter borders undergo partial volume effects. Regional atrophy that increases the amount of neighboring CSF accentuates these partial volume effects. Application of partial volume correction to amyloid PET is expected to increase the amyloid PET deposition in atrophied gray matter and lead to more accurate quantification [30, 32–34]. Partial volume correction is usually performed using segmented gray matter from three-dimensional MRI coregistered to amyloid PET images.

Cognitively normal individuals

Several autopsy studies have determined the postmortem presence of significant Aβ deposits in more than 30% of cognitively normal older individuals and concluded that the extent of the Aβ pathology may be indistinguishable from that found in AD [35, 36]. In accordance with these autopsy results, several ^{11}C-PiB PET studies have consistently detected elevated ^{11}C-PiB binding in a subset of normal older volunteers, with the proportion of "^{11}C-PiB-positive" cases ranging from 10 to 30% depending on the age of the cohort and the threshold used to define ^{11}C-PiB positivity [27, 32, 37–40]. In contrast, elevated binding has not been reported in young normal controls. A minority of older controls show a distribution pattern of ^{11}C-PiB binding that is essentially indistinguishable from that seen in AD. The high rate of ^{11}C-PiB positivity in normal controls suggests that a positive ^{11}C-PiB scan cannot be interpreted without a careful clinical evaluation and emphasizes that amyloid imaging alone must not serve as a surrogate for a clinical diagnosis of AD.

Advancing age increases the frequency of ^{11}C-PiB-positive findings in normal controls, from 18% in those aged 60–69 years to 65% in those older than 80 years [41]. The prevalence of Aβ deposition, as detected by postmortem in cognitively normal individuals, exponentially increases with advancing age. The prevalence of ^{11}C-PiB-positive normal controls increases with advancing age in a similar exponential fashion, but precedes the postmortem study by 10–15 years. Aβ deposition seems almost inevitable with advancing age. One study showed that normal controls with a parent affected by late-onset AD have increased ^{11}C-PiB deposition in brain regions typically affected in clinical AD patients compared with normal controls without family history [42]. In addition, significant parent-of-origin effects on Aβ deposition were found. Normal controls with mothers affected by late-onset AD show increased and more widespread ^{11}C-PiB deposition than those with affected fathers. Another study showed that ^{11}C-PiB deposition in normal controls correlates with the apolipoprotein E (APOE) ε4 gene dose [43]. APOE ε4, an isoform of the APOE gene in humans, is the major genetic risk factor for late-onset familial and sporadic AD [44], which account for most AD cases. APOE ε4 increases the risk and decreases the age of onset of AD in a gene dose-dependent manner [45]. APOE ε4 is present in roughly 20–25% of the human population, and APOE ε4 carriers account for 60–75% of AD cases in most clinical studies [46], highlighting the importance of APOE ε4 in AD pathogenesis.

MCI

Amyloid imaging can potentially identify patients with MCI who already show Aβ aggregation, and who are thus in the early clinical phase of AD, and can separate them from patients with alternative causes of cognitive impairment. The division of MCI patients into more biologically homogeneous groups may also facilitate their inclusion in clinical trials for AD-specific therapies, allowing these treatments to be tested in patients earlier in the disease course. Perhaps, the correct use of anti-amyloid monotherapies will be as a prophylactic given long before the onset of symptoms in people at risk of AD [47]. Numerous studies of MCI have demonstrated that ^{11}C-PiB uptake is intermediate between AD and controls. However, ^{11}C-PiB-binding levels in MCI in most studies are largely bimodal, with most cases showing an AD-like uptake level, a minority of cases having low control-level binding, and a small number falling into the intermediate range. Overall, 52–87% of MCI patients show elevated ^{11}C-PiB binding, depending on the criteria used to diagnose MCI and the threshold used to define ^{11}C-PiB positivity [29, 32, 37, 38, 48–52]. Individuals meeting criteria for amnestic MCI were more likely to be ^{11}C-PiB positive than patients with nonamnestic MCI. Villemagner et al. [32] demonstrated that the progression of MCI to AD occurred in 67% of individuals with MCI and high ^{11}C-PiB deposition versus 5% of those with low ^{11}C-PiB. Forsberg et al.

[50] reported that 33% of individuals with MCI and elevated ^{11}C-PiB binding later converted to AD in clinical follow-up. Irrespective of MCI subtypes, longitudinal follow-up work determined that 5 of the 13 amyloid-positive patients, but 0 of the 10 amyloid-negative patients converted to clinical AD [51].

AD dementia

The initial objective of amyloid PET was to detect Aβ amyloidosis in patients clinically diagnosed with AD. As expected, the vast majority of AD patients show elevated tracer deposition [17, 38, 48, 52–54]. Using clinical diagnosis as a gold standard, the sensitivity of amyloid PET for AD has been reported to be 60–100% [52, 55, 56], with most studies reporting sensitivities of 90% or greater. The proportion of negative scans in AD is very similar to the fraction of patients clinically diagnosed with AD at dementia referral centers who are subsequently found to have an alternative pathology at autopsy [57], suggesting that many amyloid PET-negative scans in AD may represent "true" negative findings. A pathology-confirmed "false-negative" amyloid PET result has been reported [58], involving a patient with Aβ plaques on frontal brain biopsy who showed low amyloid PET binding when studied with PET 20 months later. Cairns et al. [59] reported an amyloid PET-negative case with reduced $A\beta_{42}$ and elevated tau in the CSF, whose postmortem biochemical analysis met the neuropathological criteria for AD. An inverse relationship between amyloid PET tracer deposition and CSF $A\beta_{42}$ has also been reported [60]. However, low CSF levels of $A\beta_{42}$ can occur in the absence of elevated amyloid PET tracer deposition [61], possibly due to concomitant Aβ oligomer formation and/or because amyloid PET may fail to bind to certain human amyloid conformations such as diffuse nonfibrillar plaque.

Familial AD

Familial AD with different autosomal dominant mutations shows higher striatal and somewhat lower cortical tracer uptake than sporadic AD. Striatal amyloid deposition may be an early feature of familial AD [62, 63]. The pattern and degree of tracer uptake are not associated with mutation type or cognitive status. Because the cerebellum also shows somewhat higher uptake in familial AD than in sporadic AD, the pons is the preferred reference region for the quantification of amyloid burden in familial AD. Similar to autosomal dominant AD, adults with down syndrome are genetically predisposed to increased amyloid burden, because they carry three copies of the amyloid precursor protein gene, located on chromosome 21. In individuals with down syndrome, amyloid tracer uptake becomes evident from around 40 years of age and increases in spatial extent in an age-dependent manner [64]. The first brain region for increased tracer uptake is the striatum, followed by the rostral prefrontal–cingulo–parietal regions.

Suspected non-AD pathophysiology

Amyloid PET introduced a new biomarker-based concept, suspected non-AD pathophysiology (SNAP) [65–67]. The term SNAP applies to individuals with normal levels of Aβ biomarkers in the brain but abnormal levels of neurodegeneration biomarkers, similar to AD, such as hypometabolism in the temporoparietal area on ^{18}F-FDG PET, medial temporal lobe atrophy on MRI, and an elevated total CSF tau (Fig. 5). It has been applied to clinically normal individuals and to those with MCI, but is applicable to any amyloid-negative, neurodegeneration-positive individual regardless of clinical status, except when the pathology underlying the neurodegeneration can be reliably inferred from the clinical presentation. SNAP is present in about 23% of clinically normal individuals aged above 65 years and in about 25% of individuals with MCI. APOE ε4 is underrepresented in individuals with SNAP compared with amyloid-positive individuals. Clinically normal and

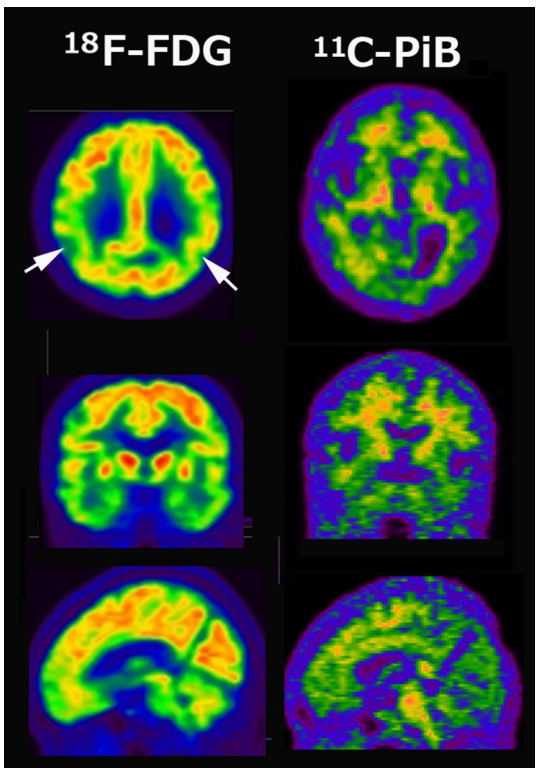

Fig. 5 Individual with suspected non-AD pathophysiology (A−/N+). ^{11}C-PiB: amyloid (A). ^{18}F-FDG: neuronal injury (N). Hypometabolism in the bilateral parietal cortex (arrows) is suggestive of AD but no Aβ load is present

mildly impaired individuals with SNAP have worse clinical and/or cognitive outcomes than individuals with normal levels of neurodegeneration and Aβ biomarkers. The AD-like hypometabolism is found in non-AD conditions, such as corticobasal degeneration, primary progressive aphasia, and cerebrovascular disease. The pattern is found even in cognitively normal individuals with increased fasting plasma glucose levels [68]. Hippocampal atrophy is a prominent feature of hippocampal sclerosis, TAR (transactive response DNA-binding protein of 43 kDa (TDP-43) pathology, argyrophilic grain disease, and anoxic-ischemic injury. TDP-43 proteinopathy in limbic brain structures is commonly observed in subjects past 80 years of age. This proteinopathy has been associated with substantial cognitive impairment that mimicked AD clinical syndrome. A new terminology: limbic-predominant age-related TDP-43 encephalopathy (LATE) has been recently proposed [69]. LATE is probably an important contributor in this group of subjects. The etiological nonspecificity of atrophy and hypometabolism observed by MRI and ^{18}F-FDG PET in areas of the brain associated with AD has given rise to the concept that the brain networks in these areas can be vulnerable to a variety of insults associated with AD, non-AD disorders, and aging.

Clinical impact

The question arises whether the use of amyloid PET is associated with a subsequent change in the management of patients with MCI or dementia of uncertain etiology. Recently, Rabinovici et al. [70] presented the first results of the Imaging Dementia-Evidence for Amyloid Scanning (IDEAS) study [71]. The study had its origins in the 2013 conclusion by the US Centers for Medicare & Medicaid Services (CMS) that the current evidence was insufficient to warrant coverage of amyloid PET scanning for routine clinical care. However, in that decision, the CMS agreed to provide coverage with evidence accumulation in studies examining whether amyloid PET improved health outcomes in Medicare and Medicaid beneficiaries. Given that no disease-modifying treatments have yet been approved, health outcomes that can be assessed at this time are those related to diagnostic test ordering, symptomatic treatment decision, or counseling. The longitudinal IDEAS study [70, 71] that included 11,409 participants with MCI or dementia of uncertain cause found a change in patient management 90 days after amyloid PET in 60.2% of patients with MCI and 63.5% of patients with dementia. Amyloid PET was associated with changes in the subsequent management of diagnostically challenging patients with cognitive disorders. Leurzy et al. [72] also reported the clinical impact of amyloid PET among memory clinic patients with an unclear diagnosis. Amyloid PET changed diagnosis in a high percentage of patients with MCI and with dementia not otherwise specified. Cholinesterase inhibitor treatment significantly increased after amyloid PET.

Tau PET

First-generation PET ligands

2-(1-{6-[(2-[Fluorine-18]fluoroethyl)(methyl)amino]-2-naphthyl}-ethylidene) malononitrile (FDDNP) is the first PET tracer to visualize AD pathology in living humans [73]. It binds to both neurofibrillary tangles (NFTs) and amyloid plaques in the brain. In the first longitudinal PET study comparing the tracer binding of ^{11}C-PiB and ^{18}F-FDDNP among AD patients, MCI patients, and healthy controls, ^{18}F-FDDNP successfully discriminated between AD and healthy controls but with a ninefold lower specific binding signal versus ^{11}C-PiB, which was thought to be due to both amyloid and tau. Interestingly, the development of ^{18}F-FDDNP opened the door to both amyloid and tau PET imaging in AD, as well as other tauopathies. It was an important milestone because postmortem histopathological studies have consistently demonstrated that NFTs are a better index of disease severity and progression than Aβ.

One of the earliest agents specifically for tau imaging was ^{11}C-labeled PBB3, a pyrinated phenyl- and pyridinyl-butadienyl-benzothiazole with a 50-fold higher affinity for tau over Aβ deposits [74]. ^{11}C-PBB3 is a PET tracer clinically used for in vivo detection of tau inclusions in AD as well as non-AD tauopathies in the human brain. However, its utility is hampered by high white matter uptake, a low target-to-white matter ratio on autoradiography in AD tissue, fast in vivo metabolism, photo-isomerization upon exposure to fluorescent light, and a dominant brain-penetrant metabolite that complicates the quantification of ligand uptake [75]. It also shows high retention in dural venous sinuses. Finally, ^{11}C labeling, with its short half-life, limits the potential use of any PET ligand compared with ^{18}F labeling. To address these issues, the ^{18}F analogues AM-PBB3 and PM-PBB3 were developed, but limited data have been published to date.

A series of quinolone derivatives have been developed at Tohoku University, ^{18}F-THK5117 [76] and ^{18}F-THK5351. Of these two, ^{18}F-THK5351 has favorable imaging characteristics, generally demonstrating higher gray matter and lower white matter uptake but lower lipophilicity [77]. It shows high affinity for the tau protein isoform with four repeats in the microtubule-binding domain (4R-tau). However, high off-target binding of ^{18}F-THK5351 was observed, especially in the thalamus, and

blocking studies with the monoamine oxidase (MAO) B inhibitor selegiline showed a dramatic 40% reduction in thalamic ^{18}F-THK5351 uptake [78]. Cortical uptake was also significantly reduced due to this off-target binding. This demonstrates that ^{18}F-THK5351 cannot be used to accurately quantify tau levels in humans in vivo.

The radioligand ^{18}F-flortaucipir (^{18}F-AV1451, T807), a benzimidazole pyrimidine derivative, is by far the most widely studied tau PET tracer [79]. It binds with high affinity to 3R and 4R tau isoforms in AD patients. Autoradiography studies using human brain tissue samples from multiple neurodegenerative disorders have largely confirmed the specific binding of ^{18}F-flortaucipir to paired helical filaments, tau-containing NFTs, and dystrophic neurites in AD brains. In comparison, ^{18}F-flortaucipir binding is absent or very low in tau aggregates composed of straight filaments as well as in alpha-synuclein or TDP-43 deposits [79, 80]. Off-target binding is observed in the choroid plexus [81, 82]. This finding is of particular interest because of the close proximity of the choroid plexus to the hippocampus, a region that is crucial in the study of AD tauopathy, because it is thought to be involved at a critical stage of AD tauopathy progression. The choroid plexus consists of a dense collection of capillaries in an ependymal stroma surrounded by a layer of epithelium. The choroid plexus of the lateral ventricles contains several materials that could possibly bind to ^{18}F-flortaucipir, including melanin, supported by the fact that Black/African American individuals show higher tracer accumulation in the choroid plexus than White American individuals [83]. Other materials found in the choroid plexus include calcification/mineralization [81], Biondi rings [84], and iron deposits [85]. This off-target binding mainly affects hippocampal ^{18}F-flortaucipir measurements, which should be interpreted with caution.

MAO has also been cited as a source of off-target binding in ^{18}F-flortaucipir PET. Vermeiren et al. [86] reported that ^{3}H-AV1451 binds in the human brain, depending on the region examined, with high affinity either to MAO-A or MAO-B. In the temporal cortex, the binding of ^{3}H-AV1451 is sensitive to clorgyline but not selegiline, indicating that most binding is to MAO-A, whereas the picture is reversed in the thalamus and subthalamic nucleus, where ^{3}H-AV1451 is equally highly sensitive to selegiline and clorgyline, indicative of substantial binding to MAO-B, in line with the known relative distribution and relative abundance of these two enzymes in the human brain. Although ^{3}H-AV1451 has about tenfold lower affinity for MAO-B than MAO-A, the levels of MAO-B in the human brain are two–tenfold higher than those of MAO-A, offsetting its lower affinity for MAO-B. On the other hand, no significant ^{18}F-flortaucipir uptake differences were observed between Parkinson's disease patients who received MAO-B inhibitors and those who did not [87]. Thus, the use of MAO-B inhibitors at pharmaceutical levels does not significantly affect ^{18}F-flortaucipir binding. Thus, MAO-B does not appear to be a significant binding target of ^{18}F-flortaucipir in clinical studies.

Second-generation tau PET ligands

^{18}F-RO-948 (Roche) is reported to have low lipophilicity and a rather low plasma-free fraction. Low nonspecific binding was shown using autoradiography in tissue from healthy controls, as well as a high gray/white matter ratio in tissue samples from AD patients with tau pathology corresponding to Braak stage V. No significant binding was observed in vitro in progressive supranuclear palsy, corticobasal disease, and Pick disease tissue samples. Thus, autoradiographic studies indicate that ^{18}F-RO-948 binds with high affinity to tau aggregated in AD brain sections, whereas lower reactivity is observed in non-AD tauopathies, suggesting that ^{18}F-RO-948 primarily recognizes a mixture of 3R and 4R tau isoforms [88]. In contrast to ^{18}F-flortaucipir, ^{18}F-RO-948 has excellent kinetic properties and appears to be free of off-target retention in the basal ganglia, thalamus, and choroid plexus. In addition, it lacks affinity for MAO-A and -B. However, off-target ^{18}F-RO-948 retention was observed in the substantia nigra and in the cerebellar vermis in two young control individuals [89]. The former could be ascribed to its binding to neuromelanin deposits.

^{18}F-MK-6240 (Merck) has a two–fivefold higher binding potential compared with ^{18}F-flortaucipir [90]. Nonhuman primate blocking studies showed no apparent off-target binding [89]. Recent studies have determined that the binding patterns of this ligand are associated with NFT deposition [91–93]. ^{18}F-MK-6240 displays favorable kinetics with rapid brain delivery and washout. The cerebellar gray matter has low binding across individuals, showing its potential use as a reference region. A reversible two-tissue compartment model well described the time-activity curves across individuals and brain regions. Off-target binding regions included the ethmoid sinus, clivus, meninges, substantia nigra, but not the basal ganglia or choroid plexus [92].

^{18}F-GTP1 (Genentech) exhibits high affinity and selectivity for tau pathology with no measurable binding to Aβ plaques or MAO-B in AD tissues or binding to other tested proteins at an affinity predicted to impede image data interpretation. In humans, ^{18}F-GTP1 exhibits favorable dosimetry and brain kinetics and no evidence of defluorination. ^{18}F-GTP1-specific binding is observed in cortical regions of the brain predicted to contain tau pathology in AD and exhibits low (< 4%) test–retest variability [94]. Furthermore, in a cross-sectional population, the degree of

[^{18}F]-GTP1-specific binding increased with AD severity and could differentiate diagnostic cohorts.

^{18}F-PI2620 (Life Molecular Imaging) is structurally similar to ^{18}F-flortaucipir, suggesting similar binding preferences to 3R/4R tau. No binding to Aβ or MAO-A/B has been reported. Good brain uptake and fast washout have been observed in healthy mice and nonhuman primates [95].

Cognitively normal individuals

Tau imaging has consistently shown ligand retention to be largely restricted to the medial temporal lobe, with cortical findings variable and relatively low or even absent [96]. This pattern in the medial temporal lobe is consistent with the neuropathological literature and may reflect an age-related tauopathy that causes hippocampal atrophy and mild amnestic deficits that are Aβ independent. Sperling et al. [97] recently reported that higher cortical levels of Aβ and tau were both associated with greater memory decline in cognitively normal old individuals. Both Aβ and tau are necessary for memory decline in the preclinical stages of AD.

Mild cognitive impairment

Individuals with MCI with positive amyloid PET show significantly greater cortical tau PET tracer retention than cognitively normal individuals [98]. Other studies have reported that the tau PET tracer retention best discriminates MCI patients from cognitively normal individuals in the parahippocampal cortex and entorhinal cortex [99, 100].

AD dementia

Patients with AD have significantly higher levels of tau tracer retention than cognitively normal individuals in the inferior lateral temporal, posterior cingulate, and lateral parietal regions, as well as other areas, with binding matching the known regional deposition of tau pathology reported in histopathological studies. Early onset AD patients have greater tau tracer cortical retention than late-onset AD patients [101, 102]. Differences in tau patterns have also been detected according to APOE ε4 status. AD patients that carry the APOE ε4 risk allele have lower overall cortical ^{18}F-AV-1451 binding, especially in the parietal and occipital cortex, but relatively higher binding in the entorhinal cortex compared with APOE ε4-negative AD patients, with corresponding differences in atrophy patterns [103]. There is also interest in the relationship between the patterns of tau deposition assessed in vivo and the symptomatology of clinical variants of sporadic AD, such as posterior cortical atrophy, the behavioral/dysexecutive variant, and the logopenic variant of primary progressive aphasia. Case series describe the retention of ^{18}F-AV-1451 in these variants of AD, with ^{18}F-AV1451 retention most prominently in the clinically affected regions, where there is a negative association between ^{18}F-AV-1451 and ^{18}F-FDG uptake [104].

Primary age-related tauopathy

Primary age-related tauopathy (PART) is a recently described entity that can cause cognitive impairment, characterized by NFTs and tau lesions without Aβ plaques in old individuals [105]. Many autopsy studies have reported brains with NFT that are indistinguishable from those of AD, in the absence of Aβ plaques. For these "NFT+/Aβ−" brains, for which formal criteria for AD neuropathological changes are not met, the NFTs are mostly restricted to structures in the medial temporal lobe, basal forebrain, brainstem, and olfactory areas. We recently revealed negative correlation between ^{18}F-THK5351 accumulation and gray matter volume in the bilateral medial temporal lobes of amyloid-negative cognitively normal older adults [106]. Symptoms in persons with PART usually range from absent to amnestic cognitive changes, with only a minority exhibiting profound impairment. Compared with AD patients, individuals with PART show significantly slower rates of decline on measures of memory, language, and visuospatial performance [107]. They also have a lower APOE ε4 allele frequency (4.1% vs. 17.6%). PART is almost universally detectable at autopsy in elderly individuals. However, tau PET has made it possible to identify this pathological process pre-mortem. There are several congruencies between PART and SNAP. These similarities include association with normal cognition or MCI, neurodegeneration of mesial temporal lobe structures, absence of Aβ deposits, and underrepresentation of APOE ε4 allele relative to AD. Tau PET scanning in conjunction with other imaging approaches such as amyloid and vascular imaging should allow further delineation of PART as a subset of SNAP.

Clinical impact

Interestingly association was hardly found between gray matter atrophy and ^{18}F-THK5351 accumulation even after partial volume correction in AD [108, 109]. This discrepancy between ^{18}F-THK5351 deposits and gray matter atrophy suggests that ^{18}F-THK5351 load precedes atrophy. A longitudinal study on tau accumulation and atrophy in AD demonstrated ^{18}F-Flortaucipir increase in the frontal regions and atrophy predominating posterior regions [110]. This spatial difference may reflect temporal lag between tau pathology and subsequent neurodegeneration that widens in the clinical phase of the disease as tau accumulation and spread accelerate. These results suggest that tau PET appears to provide important information earlier in therapeutic trials

of AD than MRI. In addition, tau PET imaging is also an attractive imaging tool for the study of non-amnesic clinical MCI/dementia syndrome which can be established using molecular biomarkers as atypical subtypes of AD such as primary progressive aphasia, posterior cortical atrophy, and corticobasal syndrome. Tau PET accumulation closely links to clinical phenotype and better co-localized to glucose hypometabolism compared to amyloid PET [104].

Tau PET and brain connectivity

Topographical similarities between tau pathology and functional brain networks have recently been explored. In the study by Hannson et al. [111], the AD-related tau PET signal primarily overlapped with the dorsal attention network and, to a lower extent, with higher visual, limbic, and default mode network components. Tau pathology may not exclusively distribute along one particular network. Schutz et al. [112] showed an interactive effect of global Aβ and neocortical tau PET measures on functional connectivity. While hyperconnectivity in default mode and salience networks was seen in the condition with high Aβ but low levels of inferior temporal tau, hypoconnectivity was present when both global Aβ and neocortical tau were high. This finding could be interpreted as support for a phase of hyperconnectivity in Aβ-positive aging, followed by a loss of connectivity with spread of tau to neocortical regions in the progression of AD. To support this finding, connectometry measured by diffusion tensor imaging showed opposite responses to elevated global tau deposition between the amyloid-negative cognitively normal group, which showed increased tract connectivity, and the amyloid-positive AD-spectrum group, which showed decreased tract connectivity [113]. This finding indicates that tau affects structural connectivity even in cognitively normal individuals. Moreover, coexisting amyloid may be chiefly related to alterations in structural connectivity responses to tau deposition.

Conclusion

Current amyloid and tau PET findings provide further evidence to support the hypothesis that both amyloid and tau pathologies of AD are required for rapid cognitive decline during the preclinical stages of AD. Thus, the selection of individuals with evidence of higher levels of both pathologies might provide greater power in clinical trials to detect a therapeutic effect on the rate of cognitive decline, particularly over a relatively short time frame [97]. Given the association between Aβ and tau and the observation that elevated levels of neocortical tau are primarily observed in the high Aβ group, it is possible that decreased Aβ accumulation might slow memory decline by preventing further accumulation of tau. This hypothesis is being tested in several ongoing secondary prevention trials in both biomarker-at-risk [114] and genetic-at-risk [115, 116] cohorts. Amyloid and tau PET have played a crucial role in the detection and tracking of the preclinical and clinical stages of AD.

Funding This study was funded by the Brain Mapping by Integrated Neurotechnologies for Disease Studies (Brain/MINDS) project (Grant no. 18dm0207017h0005) from the Japan Agency for Medical Research and Development (AMED).

Compliance with ethical standards

Conflict of interest The authors have no conflict of interest to disclose with respect to this article.

Ethical statement This article does not contain any studies with human participants or animals performed by any of the authors.

References

1. Association Alzheimer's. 2016 Alzheimer's disease facts and figures. Alzheimers Dement. 2016;12:459–509.
2. Alzheimer's Disease International. The state of the art of dementia research: new frontiers. World Alzheimer Report. 2018: the global voice on dementia. 2018. https://www.alz.co.uk/research/world-report-2018. Accessed 21 Sept 2018.
3. Montgomery W, Ueda K, Jorgensen M, Stathis S, Cheng Y, Nakamura T. Epidemiology, associated burden, and current clinical practice for the diagnosis and management of Alzheimer's disease in Japan. Clinicoecon Outcomes Res. 2017;10:13–28.
4. McKhann G, Drachman D, Folstein M, Katzman R, Price D, Stadlan EM. Clinical diagnosis of Alzheimer's disease: report of the NINCDS-ADRDA Work Group under the auspices of Department of Health and Human Services Task Force on Alzheimer's Disease. Neurology. 1984;34:939–44.
5. McKhann GM, Knopman DS, Chertkow H, Hyman BT, Jack CR Jr, Kawas CH, et al. The diagnosis of dementia due to Alzheimer's disease: recommendations from the National Institute on Aging-Alzheimer's Association workgroups on diagnostic guidelines for Alzheimer's disease. Alzheimers Dement. 2011;7:263–9.
6. Dubois B, Feldman HH, Jacova C, Hampel H, Molinuevo JL, Blennow K, et al. Advancing research diagnostic criteria for Alzheimer's disease: the IWG-2 criteria. Lancet Neurol. 2014;13:614–29.
7. Jack CR Jr, Albert MS, Knopman DS, McKhann GM, Sperling RA, Carrillo MC, et al. Introduction to the recommendations from the National Institute on Aging-Alzheimer's Association workgroups on diagnostic guidelines for Alzheimer's disease. Alzheimers Dement. 2011;7:257–62.
8. Sperling RA, Aisen PS, Beckett LA, Bennett DA, Craft S, Fagan AM, et al. Toward defining the preclinical stages of Alzheimer's disease: recommendations from the National Institute

on Aging-Alzheimer's Association workgroups on diagnostic guidelines for Alzheimer's disease. Alzheimers Dement. 2011;7:280–92.
9. Petersen RC. Mild cognitive impairment as a diagnostic entity. J Intern Med. 2004;256:183–94.
10. Meyer J, Xu G, Thornby J, Chowdhury M, Quach M. Longitudinal analysis of abnormal domains comprising mild cognitive impairment (MCI) during aging. J Neurol Sci. 2002;201:19–25.
11. Gauthier S, Reisberg B, Zaudig M, Petersen RC, Ritchie K, Broich K, et al. International psychogeriatric association expert conference on mild cognitive impairment. Lancet. 2006;367:1262–70.
12. Albert MS, DeKosky ST, Dickson D, Dubois B, Feldman HH, Fox NC, et al. The diagnosis of mild cognitive impairment due to Alzheimer's disease: recommendations from the National Institute on Aging-Alzheimer's Association workgroups on diagnostic guidelines for Alzheimer's disease. Alzheimers Dement. 2011;7:270–9.
13. Ishikawa T, Ikeda M. Mild cognitive impairment in a population-based epidemiological study. Psychogeriatrics. 2007;7:104–8.
14. Iwatsubo T, Iwata A, Suzuki K, Ihara R, Arai H, Ishii K, et al. Japanese and North American Alzheimer's disease neuroimaging initiative studies: harmonization for international trials. Alzheimers Dement. 2018;14:1077–87.
15. Jack CR Jr, Bennett DA, Blennow K, Carrillo MC, Feldman HH, Frisoni GB, et al. A/T/N: an unbiased descriptive classification scheme for Alzheimer disease biomarkers. Neurology. 2016;87:539–47.
16. Mathis CA, Wang Y, Holt DP, Huang GF, Debnath ML, Klunk WE. Synthesis and evaluation of ^{11}C-labeled 6-substituted 2-arylbenzothiazoles as amyloid imaging agents. J Med Chem. 2003;46:2740–54.
17. Klunk WE, Engler H, Nordberg A, Wang Y, Blomqvist G, Holt DP, et al. Imaging brain amyloid in Alzheimer's disease with Pittsburgh Compound-B. Ann Neurol. 2004;55:306–19.
18. Bacskai BJ, Frosch MP, Freeman SH, Raymond SB, Augustinack JC, Johnson KA, et al. Molecular imaging with Pittsburgh Compound B confirmed at autopsy: a case report. Arch Neurol. 2007;64:431–4.
19. Ikonomovic MD, Klunk WE, Abrahamson EE, Mathis CA, Price JC, Tsopelas ND, et al. Post-mortem correlates of in vivo PiB-PET amyloid imaging in a typical case of Alzheimer's disease. Brain. 2008;131:1630–45.
20. Nelissen N, Van Laere K, Thurfjell L, Owenius R, Vandenbulcke M, Koole M, et al. Phase 1 study of the Pittsburgh Compound B derivative ^{18}F-flutemetamol in healthy volunteers and patients with probable Alzheimer disease. J Nucl Med. 2009;50:1251–9.
21. Wong DF, Rosenberg PB, Zhou Y, Kumar A, Raymont V, Ravert HT, et al. In vivo imaging of amyloid deposition in Alzheimer disease using the radioligand ^{18}F-AV-45 (florbetapir [corrected] F 18). J Nucl Med. 2010;51:913–20.
22. Barthel H, Gertz HJ, Dresel S, Peters O, Bartenstein P, Buerger K, et al. Cerebral amyloid-β PET with florbetaben (^{18}F) in patients with Alzheimer's disease and healthy controls: a multicentre phase 2 diagnostic study. Lancet Neurol. 2011;10:424–35.
23. Rowe CC, Villemagne VL. Brain amyloid imaging. J Nucl Med. 2011;52:1733–40.
24. Hanseeuw BJ, Betensky RA, Mormino EC, Schultz AP, Sepulcre J, Becker JA, et al. PET staging of amyloidosis using striatum. Alzheimers Dement. 2018;14:1281–92.
25. Fodero-Tavoletti MT, Rowe CC, McLean CA, Leone L, Li QX, Masters CL, et al. Characterization of PiB binding to white matter in Alzheimer disease and other dementias. J Nucl Med. 2009;50:198–204.
26. Logan J. Graphical analysis of PET data applied to reversible and irreversible tracers. Nucl Med Biol. 2000;27:661–70.
27. Mintun MA, Larossa GN, Sheline YI, Dence CS, Lee SY, Mach RH, et al. [^{11}C]PIB in a nondemented population: potential antecedent marker of Alzheimer disease. Neurology. 2006;67:446–52.
28. Koivunen J, Verkkoniemi A, Aalto S, Paetau A, Ahonen JP, Viitanen M, et al. PET amyloid ligand [^{11}C]PIB uptake shows predominantly striatal increase in variant Alzheimer's disease. Brain. 2008;131:1845–53.
29. Lopresti BJ, Klunk WE, Mathis CA, Hoge JA, Ziolko SK, Lu X, et al. Simplified quantification of Pittsburgh Compound B amyloid imaging PET studies: a comparative analysis. J Nucl Med. 2005;46:1959–72.
30. Mikhno A, Devanand D, Pelton G, Cuasay K, Gunn R, Upton N, et al. Voxel-based analysis of ^{11}C-PIB scans for diagnosing Alzheimer's disease. J Nucl Med. 2008;49:1262–9.
31. Klunk WE, Koeppe RA, Price JC, Benzinger TL, Devous MD Sr, Jagust WJ, et al. The Centiloid Project: standardizing quantitative amyloid plaque estimation by PET. Alzheimers Dement. 2015;11:1–15.
32. Villemagne VL, Pike KE, Chételat G, Ellis KA, Mulligan RS, Bourgeat P, et al. Longitudinal assessment of Aβ and cognition in aging and Alzheimer disease. Ann Neurol. 2011;69:181–92.
33. Sasaki K, Maikusa N, Imabayashi E, Yuasa T, Matsuda H. The feasibility of ^{11}C-PIB-PET/CT for amyloid plaque burden: validation of the effectiveness of CT-based partial volume correction. Brain Behav. 2016;6:e00532.
34. Gonzalez-Escamilla G, Lange C, Teipel S, Buchert R, Grothe MJ. Alzheimer's disease neuroimaging initiative. PETPVE12: an SPM toolbox for partial volume effects correction in brain PET—application to amyloid imaging with AV45-PET. Neuroimage. 2017;147:669–77.
35. Bennett DA, Schneider JA, Arvanitakis Z, Kelly JF, Aggarwal NT, Shah RC, et al. Neuropathology of older persons without cognitive impairment from two community-based studies. Neurology. 2006;66:1837–44.
36. Hulette CM, Welsh-Bohmer KA, Murray MG, Saunders AM, Mash DC, McIntyre LM. Neuropathological and neuropsychological changes in "normal" aging: evidence for preclinical Alzheimer disease in cognitively normal individuals. J Neuropathol Exp Neurol. 1998;57:1168–74.
37. Pike KE, Savage G, Villemagne VL, Ellis KA, Mulligan RS, Bourgeat P, et al. Beta-amyloid imaging and memory in non-demented individuals: evidence for preclinical Alzheimer's disease. Brain. 2007;130:2837–44.
38. Jack CR Jr, Lowe VJ, Senjem ML, Weigand SD, Kemp BJ, Shiung MM, et al. ^{11}C PiB and structural MRI provide complementary information in imaging of Alzheimer's disease and amnestic mild cognitive impairment. Brain. 2008;131:665–80.
39. Aizenstein HJ, Nebes RD, Saxton JA, Price JC, Mathis CA, Tsopelas ND, et al. Frequent amyloid deposition without significant cognitive impairment among the elderly. Arch Neurol. 2008;65:1509–17.
40. Mormino EC, Kluth JT, Madison CM, Rabinovici GD, Baker SL, Miller BL, et al. Episodic memory loss is related to hippocampal-mediated beta-amyloid deposition in elderly subjects. Brain. 2009;132:1310–23.
41. Rowe CC, Ellis KA, Rimajova M, Bourgeat P, Pike KE, Jones G, et al. Amyloid imaging results from the Australian Imaging, Biomarkers and Lifestyle (AIBL) study of aging. Neurobiol Aging. 2010;31:1275–83.
42. Mosconi L, Rinne JO, Tsui WH, Berti V, Li Y, Wang H, Murray J, et al. Increased fibrillar amyloid-{beta} burden in normal individuals with a family history of late-onset Alzheimer's. Proc Natl Acad Sci USA. 2010;107:5949–54.
43. Reiman EM, Chen K, Liu X, Bandy D, Yu M, Lee W, et al. Fibrillar amyloid-beta burden in cognitively normal people at 3

levels of genetic risk for Alzheimer's disease. Proc Natl Acad Sci USA. 2009;106:6820–5.
44. Kanekiyo T, Xu H, Bu G. ApoE and Aβ in Alzheimer's disease: accidental encounters or partners? Neuron. 2014;81:740–54.
45. Kim J, Basak JM, Holtzman DM. The role of apolipoprotein E in Alzheimer's disease. Neuron. 2009;63:287–303.
46. Farrer LA, Cupples LA, Haines JL, Hyman B, Kukull WA, Mayeux R, et al. Effects of age, sex, and ethnicity on the association between apolipoprotein E genotype and Alzheimer disease: a meta-analysis. JAMA J Am Med Assoc. 1997;278:1349–56.
47. St George-Hyslop PH, Morris JC. Will anti-amyloid therapies work for Alzheimer's disease? Lancet. 2008;372:180–2.
48. Rowe CC, Ng S, Ackermann U, Gong SJ, Pike K, Savage G, et al. Imaging beta-amyloid burden in aging and dementia. Neurology. 2007;68:1718–25.
49. Kemppainen NM, Aalto S, Wilson IA, Någren K, Helin S, Brück A, et al. PET amyloid ligand [^{11}C]PIB uptake is increased in mild cognitive impairment. Neurology. 2007;68:1603–6.
50. Forsberg A, Engler H, Almkvist O, Blomquist G, Hagman G, Wall A, et al. PET imaging of amyloid deposition in patients with mild cognitive impairment. Neurobiol Aging. 2008;29:1456–65.
51. Wolk DA, Price JC, Saxton JA, Snitz BE, James JA, Lopez OL, et al. Amyloid imaging in mild cognitive impairment subtypes. Ann Neurol. 2009;65:557–68.
52. Omachi Y, Ito K, Arima K, Matsuda H, Nakata Y, Sakata M, et al. Clinical impact of (11) C-Pittsburgh Compound-B positron emission tomography carried out in addition to magnetic resonance imaging and single-photon emission computed tomography on the diagnosis of Alzheimer's disease in patients with dementia and mild cognitive impairment. Psychiatry Clin Neurosci. 2015;69:741–51.
53. Ng S, Villemagne VL, Berlangieri S, Lee ST, Lee ST, Cherk M, Gong SJ, et al. Visual assessment versus quantitative assessment of ^{11}C-PIB PET and ^{18}F-FDG PET for detection of Alzheimer's disease. J Nucl Med. 2007;48:547–52.
54. Edison P, Archer HA, Hinz R, Hammers A, Pavese N, Tai YF, et al. Amyloid, hypometabolism, and cognition in Alzheimer disease: an [^{11}C]PIB and [^{18}F]FDG PET study. Neurology. 2007;68:501–8.
55. Ossenkoppele R, Prins ND, Pijnenburg YA, Lemstra AW, van der Flier WM, Adriaanse SF, et al. Impact of molecular imaging on the diagnostic process in a memory clinic. Alzheimers Dement. 2013;9:414–21.
56. Morris E, Chalkidou A, Hammers A, Peacock J, Summers J, Keevil S. Diagnostic accuracy of ^{18}F amyloid PET tracers for the diagnosis of Alzheimer's disease: a systematic review and meta-analysis. Eur J Nucl Med Mol Imaging. 2016;43:374–85.
57. Berg L, McKeel DW Jr, Miller JP, Storandt M, Rubin EH, Morris JC, et al. Clinicopathologic studies in cognitively healthy aging and Alzheimer's disease: relation of histologic markers to dementia severity, age, sex, and apolipoprotein E genotype. Arch Neurol. 1998;55:326–35.
58. Leinonen V, Alafuzoff I, Aalto S, Suotunen T, Savolainen S, Någren K, et al. Assessment of beta-amyloid in a frontal cortical brain biopsy specimen and by positron emission tomography with carbon 11-labeled Pittsburgh Compound B. Arch Neurol. 2008;65:1304–9.
59. Cairns NJ, Ikonomovic MD, Benzinger T, Storandt M, Fagan AM, Shah AR, et al. Absence of Pittsburgh Compound B detection of cerebral amyloid beta in a patient with clinical, cognitive, and CSF markers of Alzheimer disease: a case report. Arch Neurol. 2009;66:1557–622.
60. Fagan AM, Mintun MA, Mach RH, Lee SY, Dence CS, Shah AR, et al. Inverse relation between in vivo amyloid imaging load and CSF Abeta42 in humans. Ann Neurol. 2006;59:512–9.
61. Fagan AM, Head D, Shah AR, Marcus D, Mintun M, Morris JC, et al. Decreased CSF Abeta(42) correlates with brain atrophy in cognitively normal elderly. Ann Neurol. 2009;65:176–83.
62. Klunk WE, Price JC, Mathis CA, Tsopelas ND, Lopresti BJ, Ziolko SK, et al. Amyloid deposition begins in the striatum of presenilin-1 mutation carriers from two unrelated pedigrees. J Neurosci. 2007;27:6174–84.
63. Villemagne VL, Ataka S, Mizuno T, Brooks WS, Wada Y, Kondo M, et al. High striatal amyloid beta-peptide deposition across different autosomal Alzheimer disease mutation types. Arch Neurol. 2009;66:1537–44.
64. Annus T, Wilson LR, Hong YT, Acosta-Cabronero J, Fryer TD, Cardenas-Blanco A, et al. The pattern of amyloid accumulation in the brains of adults with Down syndrome. Alzheimers Dement. 2016;12:538–45.
65. Jack CR Jr, Knopman DS, Chételat G, Dickson D, Fagan AM, Frisoni GB, et al. Suspected non-Alzheimer disease pathophysiology—concept and controversy. Nat Rev Neurol. 2016;12:117–24.
66. Burnham SC, Bourgeat P, Doré V, Savage G, Brown B, Laws S, et al. Clinical and cognitive trajectories in cognitively healthy elderly individuals with suspected non Alzheimer's disease pathophysiology (SNAP) or Alzheimer's disease pathology: a longitudinal study. Lancet Neurol. 2016;15:1044–53.
67. Schreiber S, Schreiber F, Lockhart SN, Horng A, Bejanin A, Landau SM, et al. Alzheimer disease signature neurodegeneration and APOE genotype in mild cognitive impairment with suspected non-Alzheimer disease pathophysiology. JAMA Neurol. 2017;74:650–9.
68. Ishibashi K, Onishi A, Fujiwara Y, Ishiwata K, Ishii K. Relationship between Alzheimer disease-like pattern of ^{18}F-FDG and fasting plasma glucoselevels in cognitively normal volunteers. J Nucl Med. 2015;56:229–33.
69. Nelson PT, Dickson DW, Trojanowski JQ, Jack CR, Boyle PA, Arfanakis K, et al. Limbic-predominant age-related TDP-43 encephalopathy (LATE): consensus working group report. Brain. 2019;142:1503–27.
70. Rabinovici GD, Gatsonis C, Apgar C, Chaudhary K, Gareen I, Hanna L, et al. Association of amyloid positron emission tomography with subsequent change in clinical management among medicare beneficiaries with mild cognitive impairment or dementia. JAMA. 2019;321:1286–94.
71. Jack CR Jr, Petersen RC. Amyloid PET and changes in clinical management for patients with cognitive impairment. JAMA. 2019;321:1258–60.
72. Leuzy A, Savitcheva I, Chiotis K, Lilja J, Andersen P, Bogdanovic N, et al. Clinical impact of [^{18}F]flutemetamol PET among memory clinic patients with an unclear diagnosis. Eur J Nucl Med Mol Imaging. 2019;46:1276–86.
73. Shoghi-Jadid K, Small GW, Agdeppa ED, Kepe V, Ercoli LM, Siddarth P, et al. Localization of neurofibrillary tangles and beta-amyloid plaques in the brains of living patients with Alzheimer disease. Am J Geriatr Psychiatry. 2002;10:24–35.
74. Maruyama M, Shimada H, Suhara T, Shinotoh H, Ji B, Maeda J, et al. Imaging of tau pathology in a tauopathy mouse model and in Alzheimer patients compared to normal controls. Neuron. 2013;79:1094–108.
75. Hashimoto H, Kawamura K, Takei M, Igarashi N, Fujishiro T, Shiomi S, et al. Identification of a major radiometabolite of [^{11}C] PBB3. Nucl Med Biol. 2015;42:905–10.
76. Okamura N, Furumoto S, Harada R, Tago T, Yoshikawa T, Fodero-Tavoletti M, et al. Novel ^{18}F-labeled arylquinoline derivatives for noninvasive imaging of tau pathology in Alzheimer disease. J Nucl Med. 2013;54:1420–7.
77. Harada R, Okamura N, Furumoto S, Furukawa K, Ishiki A, Tomita N, et al. ^{18}F-THK5351: a novel PET radiotracer for imaging

neurofibrillary pathology in Alzheimer disease. J Nucl Med. 2016;57:208–14.
78. Ng KP, Pascoal TA, Mathotaarachchi S, Therriault J, Kang MS, Shin M, et al. Monoamine oxidase B inhibitor, selegiline, reduces ^{18}F-THK5351 uptake in the human brain. Alzheimers Res Ther. 2017;9:25.
79. Marquié M, Normandin MD, Vanderburg CR, Costantino IM, Bien EA, Rycyna LG, et al. Validating novel tau positron emission tomography tracer [F-18]-AV-1451 (T807) on postmortem brain tissue. Ann Neurol. 2015;78:787–800.
80. Sander K, Lashley T, Gami P, Gendron T, Lythgoe MF, Rohrer JD, et al. Characterization of tau positron emission tomography tracer [^{18}F]AV-1451 binding to postmortem tissue in Alzheimer's disease, primary tauopathies, and other dementias. Alzheimers Dement. 2016;12:1116–24.
81. Lowe VJ, Curran G, Fang P, Liesinger AM, Josephs KA, Parisi JE, et al. An autoradiographic evaluation of AV-1451 Tau PET in dementia. Acta Neuropathol Commun. 2016;4:58.
82. Marquié M, Verwer EE, Meltzer AC, Kim SJW, Agüero C, Gonzalez J, et al. Lessons learned about [F-18]-AV-1451 off-target binding from an autopsy-confirmed Parkinson's case. Acta Neuropathol Commun. 2017;5:75.
83. Lee CM, Jacobs HIL, Marquié M, Becker JA, Andrea NV, Jin DS, et al. ^{18}F-Flortaucipir binding in choroid plexus: related to race and hippocampus signal. J Alzheimers Dis. 2018;62:1691–702.
84. Ikonomovic MD, Uryu K, Abrahamson EE, Ciallella JR, Trojanowski JQ, Lee VM, et al. Alzheimer's pathology in human temporal cortex surgically excised after severe brain injury. Exp Neurol. 2004;190:192–203.
85. Choi JY, Cho H, Ahn SJ, Lee JH, Ryu YH, Lee MS, et al. Off-target ^{18}F-AV-1451 binding in the basal ganglia correlates with age-related iron accumulation. J Nucl Med. 2018;59:117–20.
86. Vermeiren C, Motte P, Viot D, Mairet-Coello G, Courade JP, Citron M, et al. The tau positron-emission tomography tracer AV-1451 binds with similar affinities to tau fibrils and monoamine oxidases. Mov Disord. 2018;33:273–81.
87. Hansen AK, Brooks DJ, Borghammer P. MAO-B Inhibitors do not block in vivo Flortaucipir ([^{18}F]-AV-1451) binding. Mol Imaging Biol. 2018;20:356–60.
88. Honer M, Gobbi L, Knust H, Kuwabara H, Muri D, Koerner M, et al. Preclinical evaluation of ^{18}F-RO6958948, ^{11}C-RO6931643, and ^{11}C-RO6924963 as novel PET radiotracers for imaging tau aggregates in Alzheimer disease. J Nucl Med. 2018;59:675–81.
89. Kuwabara H, Comley RA, Borroni E, Honer M, Kitmiller K, Roberts J, et al. Evaluation of ^{18}F-RO-948 PET for quantitative assessment of tau accumulation in the human brain. J Nucl Med. 2018;59:1877–84.
90. Hostetler ED, Walji AM, Zeng Z, Miller P, Bennacef I, Salinas C, et al. Preclinical characterization of ^{18}F-MK-6240, a promising PET tracer for in vivo quantification of human neurofibrillary tangles. J Nucl Med. 2016;57:1599–606.
91. Pascoal TA, Shin M, Kang MS, Chamoun M, Chartrand D, Mathotaarachchi S, et al. In vivo quantification of neurofibrillary tangles with [^{18}F]MK-6240. Alzheimers Res Ther. 2018;10:74.
92. Betthauser TJ, Cody KA, Zammit MD, Murali D, Converse AK, Barnhart TE, et al. In vivo characterization and quantification of neurofibrillary tau PET radioligand ^{18}F-MK-6240 in humans from Alzheimer disease dementia to young controls. J Nucl Med. 2019;60:93–9.
93. Lohith TG, Bennacef I, Vandenberghe R, Vandenbulcke M, Salinas CA, Declercq R, et al. Brain imaging of Alzheimer dementia patients and elderly controls with ^{18}F-MK-6240, a PET tracer targeting neurofibrillary tangles. J Nucl Med. 2019;60:107–14.
94. Sanabria Bohórquez S, Marik J, Ogasawara A, Tinianow JN, Gill HS, Barret O, et al. [^{18}F]GTP1 (Genentech Tau Probe 1), a radioligand for detecting neurofibrillary tangle tau pathology in Alzheimer's disease. Eur J Nucl Med Mol Imaging. 2019. https://doi.org/10.1007/s00259-019-04399-0.
95. Kroth H, Oden F, Molette J, Schieferstein H, Capotosti F, Mueller A, et al. Discovery and preclinical characterization of [^{18}F]PI-2620, a next-generation tau PET tracer for the assessment of tau pathology in Alzheimer's disease and other tauopathies. Eur J Nucl Med Mol Imaging. 2019. https://doi.org/10.1007/s00259-019-04397-2.
96. Maass A, Landau S, Baker SL, Horng A, Lockhart SN, La Joie R, et al. Comparison of multiple tau-PET measures as biomarkers in aging and Alzheimer's disease. Neuroimage. 2017;157:448–63.
97. Sperling RA, Mormino EC, Schultz AP, Betensky RA, Papp KV, Amariglio RE, et al. The impact of amyloid-beta and tau on prospective cognitive decline in older individuals. Ann Neurol. 2019;85:181–93.
98. Chiotis K, Saint-Aubert L, Savitcheva I, Jelic V, Andersen P, Jonasson M, et al. Imaging in-vivo tau pathology in Alzheimer's disease with THK5317 PET in a multimodal paradigm. Eur J Nucl Med Mol Imaging. 2016;43:1686–99.
99. Cho H, Choi JY, Hwang MS, Lee JH, Kim YJ, Lee HM, et al. Tau PET in Alzheimer disease and mild cognitive impairment. Neurology. 2016;87:375–83.
100. Johnson KA, Schultz A, Betensky RA, Becker JA, Sepulcre J, Rentz D, et al. Tau positron emission tomographic imaging in aging and early Alzheimer disease. Ann Neurol. 2016;79:110–9.
101. Cho H, Choi JY, Hwang MS, Kim YJ, Lee HM, Lee HS, et al. In vivo cortical spreading pattern of tau and amyloid in the Alzheimer disease spectrum. Ann Neurol. 2016;80:247–58.
102. Pontecorvo MJ, Devous MD Sr, Navitsky M, Lu M, Salloway S, Schaerf FW, et al. Relationships between flortaucipir PET tau binding and amyloid burden, clinical diagnosis, age and cognition. Brain. 2017;140:748–63.
103. Mattsson N, Ossenkoppele R, Smith R, Strandberg O, Ohlsson T, Jögi J, et al. Greater tau load and reduced cortical thickness in APOE ε4-negative Alzheimer's disease: a cohort study. Alzheimers Res Ther. 2018;10:77.
104. Ossenkoppele R, Schonhaut DR, Schöll M, Lockhart SN, Ayakta N, Baker SL, et al. Tau PET patterns mirror clinical and neuroanatomical variability in Alzheimer's disease. Brain. 2016;139:1551–677.
105. Crary JF, Trojanowski JQ, Schneider JA, Abisambra JF, Abner EL, Alafuzoff I, et al. Primary age-related tauopathy (PART): a common pathology associated with human aging. Acta Neuropathol. 2014;128:755–66.
106. Shigemoto Y, Sone D, Ota M, Maikusa N, Ogawa M, Okita K, et al. Voxel-based comparison of ^{18}F-THK5351 accumulation and gray matter volume in the brain of cognitively normal older adults. EJNMMI Res 2019;9:81.
107. Bell WR, An Y, Kageyama Y, English C, Rudow GL, Pletnikova O, et al. Neuropathologic, genetic, and longitudinal cognitive profiles in primary age-related tauopathy (PART) and Alzheimer's disease. Alzheimers Dement. 2019;15:8–16.
108. Sone D, Imabayashi E, Maikusa N, Okamura N, Furumoto S, Kudo Y, et al. Regional tau deposition and subregion atrophy of medial temporal structures in early Alzheimer's disease: a combined positron emission tomography/magnetic resonance imaging study. Alzheimers Dement (Amst). 2017;9:35–40.
109. Shigemoto Y, Sone D, Imabayashi E, Maikusa N, Okamura N, Furumoto S, et al. Dissociation of tau deposits and brain atrophy in early Alzheimer's disease: a combined positron emission tomography/magnetic resonance imaging study. Front Aging Neurosci. 2018;10:223.
110. Harrison TM, La Joie R, Maass A, Baker SL, Swinnerton K, Fenton L, et al. Longitudinal tau accumulation and atrophy in aging and alzheimer disease. Ann Neurol. 2019;85:229–40.

111. Hansson O, Grothe MJ, Strandberg TO, Ohlsson T, Hägerström D, Jögi J, et al. Tau pathology distribution in Alzheimer's disease corresponds differentially to cognition-relevant functional brain networks. Front Neurosci. 2017;11:167.
112. Schultz AP, Chhatwal JP, Hedden T, Mormino EC, Hanseeuw BJ, Sepulcre J, et al. Phases of hyperconnectivity and hypoconnectivity in the default mode and salience networks track with amyloid and tau in clinically normal individuals. J Neurosci. 2017;37:4323–31.
113. Shigemoto Y, Sone D, Maikusa N, Okamura N, Furumoto S, Kudo Y, et al. Association of deposition of tau and amyloid-β proteins with structural connectivity changes in cognitively normal older adults and Alzheimer's disease spectrum patients. Brain Behav. 2018;8:e01145.
114. Sperling RA, Rentz DM, Johnson KA, Karlawish J, Donohue M, Salmon DP, et al. The A4 study: stopping AD before symptoms begin? Sci Transl Med. 2014;6:228fs13.
115. Bateman RJ, Aisen PS, De Strooper B, Fox NC, Lemere CA, Ringman JM, et al. Autosomal-dominant Alzheimer's disease: a review and proposal for the prevention of Alzheimer's disease. Alzheimers Res Ther. 2011;3:1.
116. Langbaum JB, Fleisher AS, Chen K, Ayutyanont N, Lopera F, Quiroz YT, et al. Ushering in the study and treatment of preclinical Alzheimer disease. Nat Rev Neurol. 2013;9:371–81.